A Comparison of the Annular Phased Array to Helical Coil Applicators for Limb and Torso Hyperthermia

MARK J. HAGMANN, MEMBER, IEEE, RONALD L. LEVIN, AND PAUL F. TURNER, MEMBER, IEEE

Abstract—**The BSD annular phased array (APA) and miniature annular phased array (MAPA) have been compared to helical coil applicators designed for the trunk and thigh, respectively. All four applicators were tested using both cylindrical saline phantoms and a phantom-filled mannequin. Patterns of deposition were determined using both an implantable electric field probe and local values of the rate of temperature increase. Scattered fields were measured when the APA and trunk helix were used with the phantom-filled mannequin.**

Deposition with the trunk helix was mainly superficial and highly heterogeneous, showing the effect of proximity of the individual turns. Deeper heating observed with the thigh helix is attributed to its greater ratio of length to diameter (L/D = 1.57 compared to the trunk helix with L/D = 1.0). Strong fields were measured external to the helical coil applicators, and tests with the mannequin suggest that the genitals could be injured if a helix was used to treat the thigh. By contrast, the BSD APA and MAPA produced deep heating and did not have strong fields external to the applicators.

I. Introduction

HYPERTHERMIA offers considerable promise as an adjuvant to cancer therapy [1]. Many different systems have been proposed for using electromagnetic energy to induce hyperthermia, but there has been great difficulty in heating deep-seated tumors. Recently, there has been much interest in helical coil applicators since some experiments have shown them to produce relatively uniform deposition over the cross section of cylindral fat–muscle phantom models of the human arm and thigh [2]. If the design parameters are properly chosen, the electric field of a long helical coil will be predominantly axial in orientation and relatively uniform over the cross section of the coil [3]. An incident field with these properties is conducive to the observed pattern of deep, relatively uniform deposition. Analyses have also been presented which are consistent with the data for long, untapered cylindral phantoms [4].

The BSD annular phased array (APA) has been shown to produce similar patterns of deposition in long cylindrical phantoms [5]. The patterns of deposition with the APA were found to be much more complex when phantoms having a more realistic mannequin shape were used in place of long cylinders [5], [6]. In clinical applications, it has been found necessary to use a bolus to limit the extent of deposition within the body. Bolusing has not been thought to be necessary with helical coil applicators, but tests of the effects of realistic body shapes have not been described prior to this paper.

The experiments described in the following sections of this paper were made in order to characterize the helical coil prior to possible clinical usage. Design parameters for the coils were chosen in order to facilitate comparision to the commercially available APA systems.

II. Description of Applicators

The APA has been described previously [6]. It consists of 16 apertures, 8 at either end of an octagonal structure which surrounds the patient. Each aperture radiates inward to generate a cylindrically convergent wave which is predominantly polarized parallel with the axis of the body. The APA has a length of about 46 cm and an inside diameter of approximately 50 cm. A bolus filled with distilled water fills the space between the APA and the patient.

The miniature annular phased array (MAPA) is a new product of the BSD Medical Corp. and is intended for use in limb hyperthermia. The MAPA is a cylindral shell having a length of about 32 cm and an inside diameter of approximately 30 cm. Eight radiating elements are contained within the shell which is approximately 1 cm in thickness. It is recommended that the MAPA also be used with a water bolus.

Two different helical coil applicators were constructed for trunk and thigh hyperthermia. The lengths of these applicators were chosen to be similar to those of the corresponding APA and MAPA in order to provide comparable axial confinement of the energy deposition. It has been shown experimentally that the magnitude of the length to diameter ratio (L/D) of a helical coil applicator must not be small if deep heating is desired [2]. For this reason, the diameters of the two helical coil applicators were chosen to be the smallest possible consistent with reasonable clearance of the trunk and thigh. The trunk helix had a length of 43 cm and a diameter of 43 cm (L/D = 1.0). The thigh helix had a length of 36 cm and a diameter of 23 cm (L/D = 1.57).

Unlike the APA and MAPA, the helical coil applicators are resonant devices and must be operated at a frequency which is dependent upon the loading in addition to the

Manuscript received August 20, 1984; revised November 30, 1984. The opinions in this paper are solely those of the authors and do not necessarily reflect official HHS opinion. Mention of trade names of commercial products does not constitute endorsement or recommendation for use by HHS.

M. J. Hagmann and R. L. Levin are with the Biomedical Engineering and Instrumentation Branch, Division of Research Services, National Institutes of Health, Bethesda, MD 20205.

P. F. Turner is with BSD Medical Corporation, Salt Lake City, UT 84108.

0018-9294/85/1100-0916$01.00

design parameters of the coil. Others have chosen to operate helical coil applicators near the FCC-assigned instrument, scientific, and medical (ISM) bands centered at 13.56, 27.12, and 40.68 MHz in order to minimize possible interference to communications [2]. In the present study, we have chosen to operate at somewhat higher frequencies with the intent of making a more direct comparison to the APA and MAPA. The choice of operating frequencies was also motivated by recent experiments which suggest that the higher frequencies used with the APA and MAPA are required for penetration into inhomogeneous internal structures such as tumors that have spread into bone [7]. It was necessary to use relatively large pitch angles in order to permit resonant operation of the coils at the higher frequencies. Our analyses suggest that when both frequency and pitch angle are changed in such a manner that resonant operation is maintained, there is little change in the depth of heating since the effects of the changes in the two variables tend to compensate [4]. Increasing the pitch angle reduces the length of wire in the helix and hence requires that the frequency be increased. By itself, the increase in frequency would tend to decrease the depth of heating. Increasing the pitch angle also reduces the number of turns on the coil which reduces the strength of the axial magnetic field and therefore also reduces the magnitude of the azimuthal electric field. Since the azimuthal electric field causes only shallow heating, this second effect of increasing the pitch angle tends to compensate for the effect of the required increase in frequency. We do not claim to have fully optimized the values of frequency and pitch angle for the two coils which were tested, but it is anticipated that the tendency for compensation would limit the improvement that could be obtained by further optimization. We are not aware of attempts by others to optimize helical coil applicators having relatively small values of L/D.

The helical coils were used at full-wave resonance (wavelength of propagation on the helix approimately equal to helix length). Others have reported that half-wave operation may provide more nearly uniform transverse heating than is obtained with full wave, but half-wave operation would require that the coil length be reduced by a factor of $\frac{2}{3}$ for the same axial effective heating length [2].

Both helical coils were wound with copper foil rather than wire since our earlier studies have shown that, for large pitch angles, the coupling efficiency is increased by the use of metal foil [8]. The trunk helix was wound with 3 turns of 4.4 cm wide foil, and the thigh helix was wound using 5 turns of 3.6 cm wide foil.

At full-wave resonance both coils have a purely resistive impedance of approximately 30 Ω when loaded with the phantoms described in this paper. This load impedance provides a reasonably good match to a standard 50 Ω feed. Since the helical coil applicators act as balanced loads, a split-tube BALUN [9] was used to allow coupling them to the unbalanced coaxial feed line. Before the BALUN was included in the circuit, strong fields were measured near the feed cable and both the resonant frequency and the pattern of deposition in a phantom were found to depend on the length of the feed cable. A BALUN was not used in the experiments reported earlier by others when helical coil applicators were operated in the full-wave mode [2].

III. Tests with Cylindrical Saline Phantoms

All four applicators were tested using a phantom consisting of a dielectric cylinder containing saline. Local values of the three orthogonal components of the electric field intensity were measured within the saline using an implantable probe made by the BSD Medical Corp. [6]. These values were then used to calculate the local deposition in the phantom.

With all applicators except the MAPA, the cylinder was filled with saline that was approximately 0.056 N (0.33 percent NaCl by weight). From 50 to 80 MHz, the calculated values of the dielectric constant and conductivity of this solution are approximately 79.0 and 0.52 S/M, respectively [10]. A more concentrated solution of approximately 0.078 N (0.45 percent NaCl by weight) was required for the higher frequencies used with the MAPA. At a frequency of 175 MHz, the calculated values of the dielectric constant and conductivity of this solution are approximately 78.5 and 0.73 S/M, respectively [10]. The dielectric properties of both solutions were verified experimentally using a method described previously [6].

The conductivity of these two solutions was chosen to be approximately two-thirds that of muscle tissue at the respective frequencies [11], [12], so that they would be fairly representative of the volume average of tissue properties within a human limb or torso. The values of dielectric constant are less appropriate—that for the more concentrated solution being about one-half that required for two-thirds muscle. It should be noted that while there were errors in the dielectric properties, the saline phantom had values of wavelength and depth of penetration that were within 24 percent of those of two-thirds muscle at all frequencies for which they were used.

Fig. 1 shows the trunk helix used with the cylindrical saline phantom. In tests made using this system, the cylinder containing the saline was made of 5 mm thick polyethylene and had a length of 51 cm and a diameter of 32 cm. It was filled to a depth of 44 cm with saline. The implantable field probe was used for measurements at 5 cm intervals both along the axis of the cylindrical phantom and along four parallel lines located near the surface of the phantom having an azimuthal spacing of 90°. A frequency of 72.64 MHz with a forward power of 40 W (1.2 W reflected) was used in this series of tests. The resulting local values of specific absorption rate (SAR, defined as rate of energy deposition per unit mass) are shown in Table I. All values have been normalized relative to the mean for measurements on the axis. The value $Z = 0$ corresponds to the base of the column of saline as well as the lower end of the applicator. Values at $\theta = 180°$ correspond to locations near the feed point of the applicator. The data of Table I have been plotted in Fig. 2. The dotted curves, numbered 1–4, represent locations with $\theta = 0°$ to

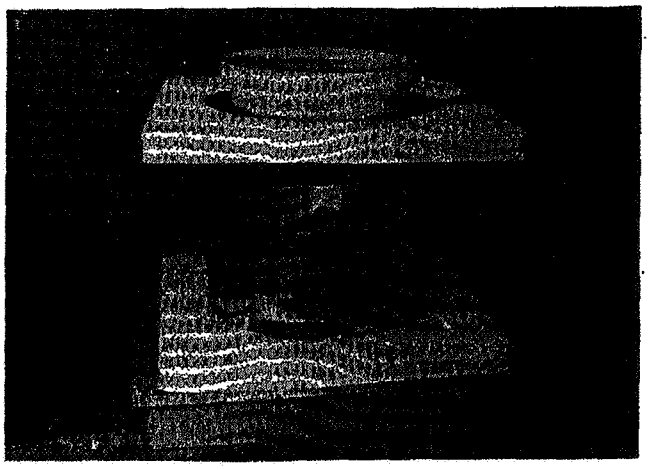

Fig. 1. Trunk helix with cylindrical saline phantom.

TABLE I
SAR DISTRIBUTION FOR TRUNK HELIX WITH SALINE PHANTOM

Z cm	Values near the phantom surface				Center
	$\theta=0^\circ$	$\theta=90^\circ$	$\theta=180^\circ$	$\theta=270^\circ$	
0	6.3	0.3	7.4	1.1	1.1
5	7.7	0.4	10.2	2.8	1.1
10	2.2	1.9	10.1	2.1	1.2
15	3.4	4.5	14.6	0.7	1.3
20	10.3	7.1	17.1	7.0	1.4
25	4.8	4.3	16.5	5.1	1.1
30	1.0	2.3	11.0	1.0	0.7
35	0.4	13.0	7.1	4.1	0.5
40	0.2	10.1	18.3	2.5	0.6
Mean	4.0	4.9	12.5	2.9	(1.00)

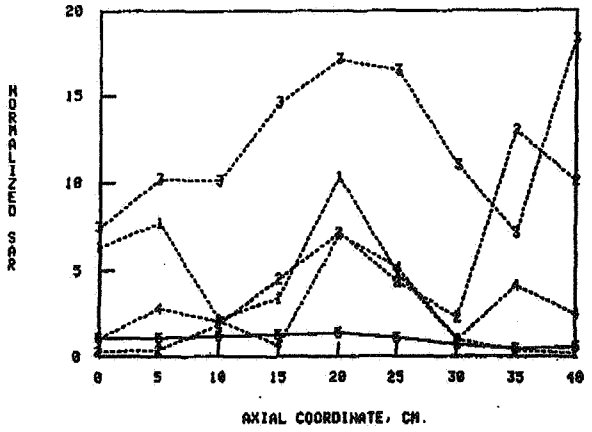

Fig. 2. SAR distribution for trunk helix with saline phantom. Axial locations are solid and surface locations are dotted.

270°, respectively. The solid line, curve 5, represents the axial locations. The mean deposition near the surface of the phantom was about 6.1 times that on the axis. The pattern of deposition near the surface of the phantom was highly heterogeneous, showing the effects of proximity of the individual turns. Averaging all 36 locations near the surface of the phantom, the total deposition was approximately 44 percent from axial, 53 percent from azimuthal, and 3 percent from radial electric fields.

In tests made with the APA, the cylinder containing the saline was made of 3 mm thick neoprene and had a length

TABLE II
SAR DISTRIBUTION FOR APA WITH SALINE PHANTOM

Z cm	Values near the phantom surface				Center
	$\theta=0^\circ$	$\theta=90^\circ$	$\theta=180^\circ$	$\theta=270^\circ$	
0	0.14	0.11	0.11	0.14	0.00
5	0.54	0.63	0.47	0.74	0.32
10	1.04	1.24	0.90	1.33	0.83
15	1.58	1.92	1.33	1.85	1.42
20	2.03	2.17	1.57	2.21	1.85
25	2.05	2.32	1.73	2.21	1.92
30	1.90	2.02	1.57	2.12	1.72
35	1.44	1.58	1.20	1.51	1.17
40	0.88	0.93	0.68	0.97	0.59
45	0.36	0.41	0.32	0.29	0.18
Mean	1.20	1.33	0.99	1.34	(1.00)

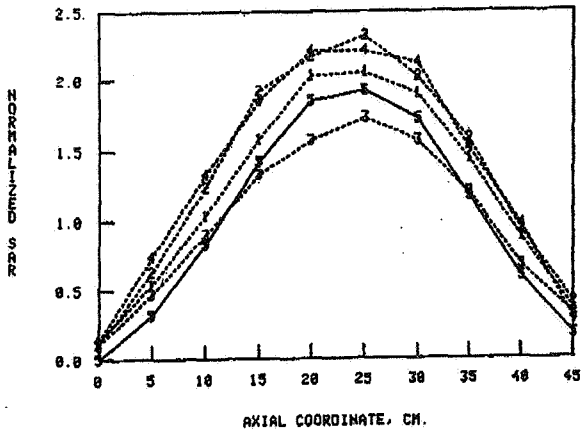

Fig. 3. SAR distribution for APA with saline phantom. Axial locations are solid and surface locations are dotted.

of 57 cm and a diameter of 33 cm. It was filled to a depth of 53 cm with saline. A thin PVC liner was used for the water-filled bolus between the APA and the cylinder. The implantable field probe was used for measurements along the axis and along four parallel lines located near the surface of the phantom, as was done with the thigh helix. A frequency of 72.63 MHz with a forward power of 40 W (0.6 W reflected) was used in this series of tests. The resulting values of normalized SAR are shown in Table II and plotted in Fig. 3 using the same conventions as in Fig. 2. The mean deposition near the surface of the phantom was about 20 percent greater than that on the axis. Averaging all 40 locations near the surface of the phantom, the total deposition was approximately 89 percent from axial and 11 percent from radial electric fields. Measured values of the azimuthal electric field were near zero when the leads of the implantable field probe were parallel to the strong axial component. This suggests that errors due to pickup by the leads were negligible under the conditions of these experiments.

In tests made with the thigh helix, the cylinder containing the saline was made of 2 mm thick polyethylene and had a length of 46 cm and a diameter of 15 cm. It was filled to a depth of 43 cm with saline. The implantable field probe was used for measurements along the axis and along four parallel lines located near the surface of the phantom, as was done with the other applicators. A frequency of 52.78 MHz with a forward power of 10 W (0.3

TABLE III
SAR DISTRIBUTION FOR THIGH HELIX WITH SALINE PHANTOM

Z cm	Values near the phantom surface				Center
	$\theta=0^\circ$	$\theta=90^\circ$	$\theta=180^\circ$	$\theta=270^\circ$	
0.0	0.08	0.00	0.17	0.06	0.06
2.5	0.28	0.08	0.36	0.22	0.19
5.0	0.47	0.30	0.58	0.55	0.44
7.5	0.86	0.53	1.08	0.86	0.69
10.0	1.52	1.47	1.77	1.41	1.11
12.5	2.58	2.47	2.27	2.25	1.58
15.0	3.41	3.41	3.44	3.08	1.89
17.5	4.24	3.99	3.94	3.60	2.05
20.0	4.10	4.10	4.02	4.02	1.91
22.5	3.58	3.63	3.52	3.41	1.56
25.0	2.77	2.99	2.25	2.50	1.19
27.5	1.69	1.94	1.50	1.52	0.72
30.0	0.94	1.19	0.97	0.67	0.50
32.5	0.33	0.17	0.36	0.25	0.11
Mean	1.92	1.88	1.87	1.74	(1.00)

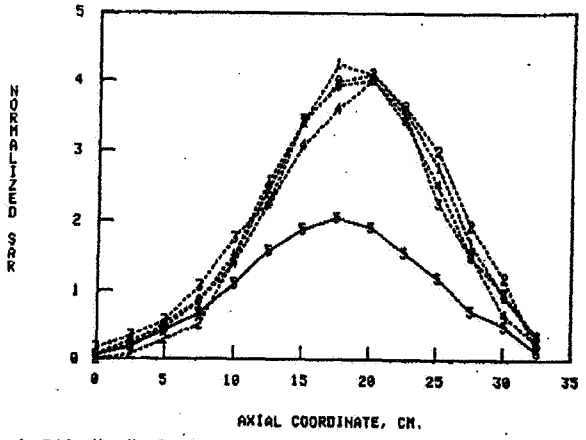

Fig. 4. SAR distribution for thigh helix with saline phantom. Axial locations are solid and surface locations are dotted.

W reflected) was used in this series of tests. The resulting values of normalized SAR are shown in Table III and plotted in Fig. 4 using the same conventions as in Fig. 2. The mean deposition near the surface of the phantom was about 1.9 times that on the axis. The pattern of deposition near the surface of the phantom shows considerably less variability than that determined for the trunk helix. Averaging all 56 locations near the surface of the phantom, the total deposition was approximately 56 percent from axial, 40 percent from azimuthal, and 4 percent from radial electric fields. The thigh helix had both a lower ratio of surface to axial deposition and a lower fraction of the total deposition caused by the azimuthal electric field than was noted for the trunk helix. It is reasonable that these two properties should occur together since the deposition due to the azimuthal electric field is approximately quadratic with radial distance from the axis [13]. This improvement in performance is thought to be caused by the larger ratio of length to diameter of the thigh helix.

Tests made with the MAPA used the same phantom as was used with the thigh helix; but the saline was more concentrated for use at the higher frequencies as noted above. Also a water-filled bolus was used between the MAPA and the phantom. The implantable field probe was used for measurements along the axis and along four parallel lines located near the surface of the phantom, as was

TABLE IV
SAR DISTRIBUTION FOR MAPA WITH SALINE PHANTOM

Z cm	Values near the phantom surface				Center
	$\theta=0^\circ$	$\theta=90^\circ$	$\theta=180^\circ$	$\theta=270^\circ$	
0.0	0.31	0.07	0.09	0.12	0.02
2.5	0.76	0.31	0.24	0.14	0.38
5.0	1.47	0.57	0.54	0.47	1.06
7.5	2.13	0.71	0.90	0.73	1.68
10.0	2.25	0.66	1.14	1.09	2.11
12.5	2.22	0.57	1.04	0.78	1.75
15.0	1.75	0.40	0.92	0.57	1.51
17.5	1.11	0.21	0.66	0.28	1.09
20.0	0.71	0.14	0.38	0.14	0.71
22.5	0.31	0.09	0.19	0.05	0.43
25.0	0.14	0.09	0.09	0.05	0.26
Mean	1.20	0.35	0.56	0.40	(1.00)

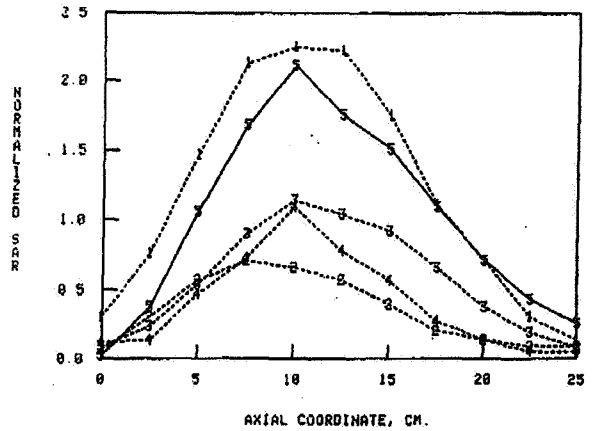

Fig. 5. SAR distribution for MAPA with saline phantom. Axial locations are solid and surface locations are dotted.

TABLE V
DEPENDENCE OF NORMALIZED SAR DISTRIBUTION ON HORIZONTAL DISPLACEMENT OF MAPA WITH SALINE PHANTOM AT Z = 10 CM

X cm	Values near the phantom surface				Center
	$\theta=0^\circ$	$\theta=90^\circ$	$\theta=180^\circ$	$\theta=270^\circ$	
0.0	2.25	0.66	1.14	1.09	2.11
2.0	1.11	0.73	1.59	0.97	1.90
4.0	1.94	0.71	1.66	1.18	2.25

done with the other applicators. A frequency of 175.14 MHz with a forward power of 10 W (<0.05 W reflected) was used in this series of tests. The resulting values of normalized SAR are shown in Table IV and plotted in Fig. 5 using the same conventions as in Fig. 2. The mean deposition near the surface of the phantom was about 63 percent of that on the axis. Averaging all 44 locations near the surface of the phantom, the total deposition was approximately 97 percent from axial and 3 percent from radial electric fields. Measured values of the azimuthal electric field were near zero, as was also found with the APA.

Table V shows the dependence of the distribution of SAR on horizontal displacement of the cylindrical phantom relative to the MAPA. The data are given for a height (Z) of 10 cm which is where the SAR was greatest for no displacement, as shown in Table IV. SAR normalization is the same as that in Table IV and the first line of Table V (X = 0.0 cm) is necessarily identical to the fifth line of Table IV (Z = 10.0 cm) as it corresponds to geometrical

TABLE VI
DIELECTRIC PHANTOM MIXTURE

Water	71.10%
Polyethylene Powder	18.31
TX-150 (gelling agent)*	10.18
NaCl	0.37
NaN_3	0.04

*Oil Center Research, Lafayette, LA.

centering of the cylindrical phantom within the MAPA. Horizontal displacements (X) of 2.0 and 4.0 cm correspond to movement of the cylindral phantom away from the feed point of the MAPA ($\theta = 180°$). A displacement of 2 cm from geometric centering decreased the relative SAR at $\theta = 0°$ from 2.25 to 1.11 since that location was now further from the maximum near the center of the MAPA. A further increase in the displacement to 4 cm caused an increase in the relative SAR at $\theta = 0°$ since that location was now quite close to one of the radiating elements of the MAPA. The dependence of SAR distribution on displacements as little as 2 cm was noted in earlier testing with the APA [6]. For this reason, it is common practice to use electric field probes to verify that the location of a patient in an APA is optimum, and such techniques would also appear to be necessary with the MAPA. The results in Table V suggest that we could have obtained more even heating near the surface of cylindrical phantom than is shown in Table IV if the position of the cylindrical phantom within the MAPA had been optimized.

IV. TESTS WITH A PHANTOM-FILLED MANNEQUIN

Local values of the electric field intensity and rate of temperature rise were determined using a phantom-filled male mannequin used in earlier testing at BSD [5], [6]. The mannequin provided a good representation of the external shape of the human body except that there were no arms and the legs were truncated at the knees. A series of thin-walled 16-gauge Teflon catheters was carefully positioned within the mannequin to allow placement of probes for measurement of both temperature and electric field strength.

The mannequin was made of thin-walled Fiberglas and was filled with a phantom mixture given in Table VI. The mixture is similar to those described earlier by others [14]. The sodium azide was added to increase the stability of the gel. The phantom mixture was found to have a dielectric constant of 68 and a conductivity of 0.47 S/M at 70 MHz. These values are approximately two-thirds those of muscle [11], [12] for simulation of mean tissue properties.

Since a helical coil applicator acts as a balanced load, it is proper to use a BALUN for coupling to an unbalanced coaxial feed line. Several difficulties were encountered in a series of tests made in which the trunk helix and phantom-filled mannequin were used without a BALUN. Electric fields as intense as 300 V/M were measured close to the feed cable for an input power of only 20 W. A single vertical catheter track was located so that it passed through the centroid of each horizontal cross section of the mannequin from the crown of the head to the crotch. The implantable electric field probe was moved along this track while it was oriented so as to measure the vertical component of the electric field intensity. These measurements showed that the ratio of the square of the vertical component of the electric field (approximately the SAR) in the neck to that in the center of the abdomen varied from 0.19 to 2.6 when the length of the coaxial feed line was changed. The resonant frequency was also found to be dependent upon cable length. A split-tube BALUN [9] was used with the helical coil applicators in the tests described in the following parts of this paper and then none of these problems were present. A BALUN was not used in the experiments reported earlier by others when helical coil applicators were operated in the full-wave mode [2].

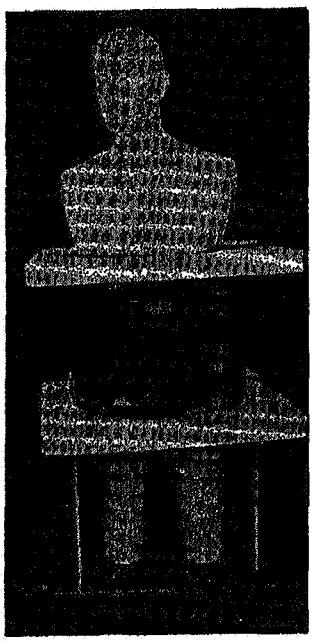

Fig. 6. Trunk helix with phantom-filled mannequin.

Tests were made using the trunk helix with the phantom-filled mannequin (with a BALUN) as shown in Fig. 6. First, the ratio of the square of the vertical component of the electric field (approximately the SAR) in the neck to that in the midabdomen was measured using the implantable electric field probe. At a frequency of 70.92 MHz, the ratio was found to be 0.70 and did not vary with changes in length of the feed line unlike earlier results before the BALUN was used.

Next the local rates of heating were determined at many locations within the mannequin to further define the pattern of energy deposition with the trunk helix. The BSD-200 thermometry system using probes developed by Bowman [15] was used for all temperature measurements. Figs. 7 and 8 show local temperature increases measured for 2 min of heating with a net power of 775 W (1000 W forward, 225 reflected) at 70.86 MHz. Fig. 7 is a front view showing values for probes positioned half-way between the front and back surfaces of the mannequin. Fig. 8 is a side view for which the probes were located in the

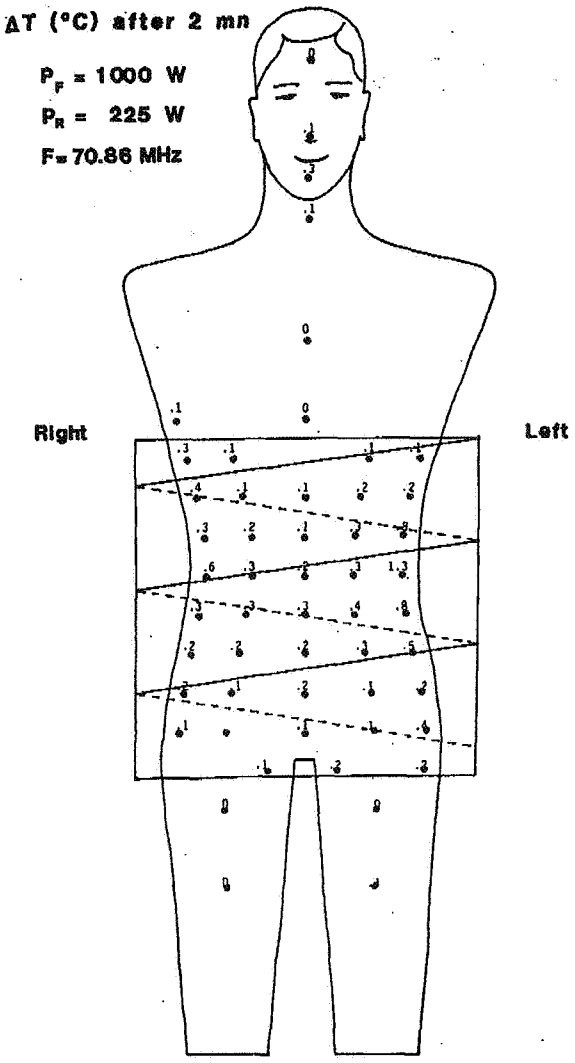

Fig. 7. Temperature change for trunk helix with mannequin.

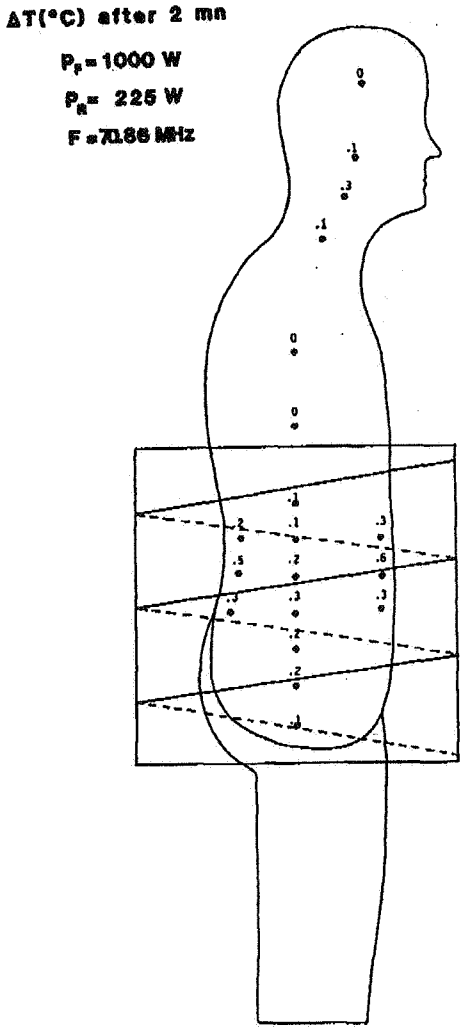

Fig. 8. Temperature change for trunk helix with mannequin.

plane of symmetry of the mannequin. The local deposition at some points near the surface of the mannequin was as much as 4 times the greatest value on the axis. This observation of excessive surface heating is consistent with the results obtained using the saline phantom. It was noted previously in this paper that the pattern of deposition with the saline phantom was highly heterogeneous, showing the effects of proximity of the individual turns of the trunk helix. The lack of symmetry in Fig. 7 is also attributed to the proximity of the individual turns, since rotating the mannequin within the helix changed the values of temperature increase at the locations closest to the surface of the mannequin.

The phantom-filled mannequin was also used with the APA, as shown in Fig. 9. First, the implantable electric field probe was used to measure the ratio of the square of the vertical component of the electric field (approximately the SAR) in the neck to that in the midabdomen. At a frequency of 82.40 MHz, this ratio was found to be 1.8 before the bolus was filled and 0.11 after it was filled.

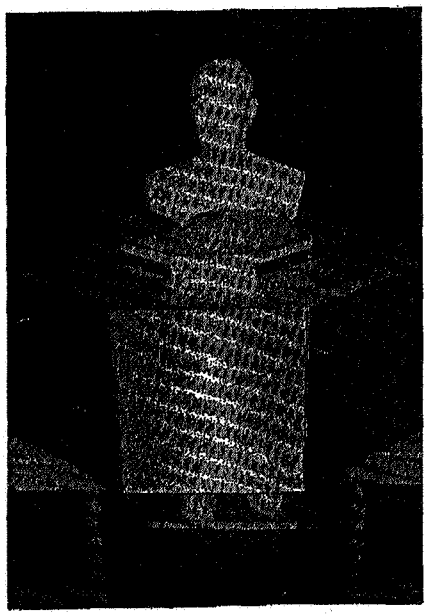

Fig. 9. APA with phantom-filled mannequin.

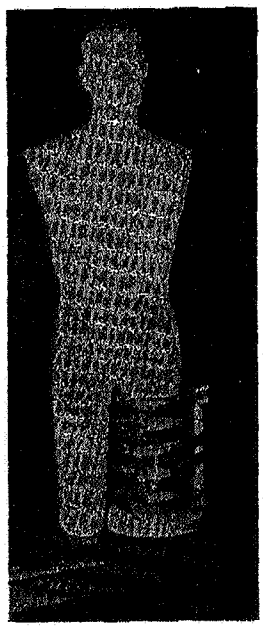

Fig. 10. Thigh helix with phantom-filled mannequin.

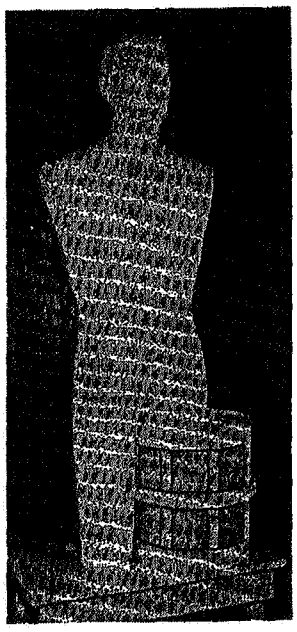

Fig. 11. MAPA with phantom-filled mannequin.

These observations are consistent with earlier studies [5] and show the need for a bolus to provide axial confinement of the fields. The bolus was used in all subsequent tests made with the APA.

Next the temperature increase was measured at several points for 2 min of heating with a net power of 775 W (800 W forward, 25 W reflected) at 70.83 MHz. These conditions were chosen to permit comparison to the trunk helix data in Figs. 7 and 8. The APA caused significantly greater deposition near the body axis than was obtained with the trunk helix. For example, a temperature increase of 0.9°C was observed at the center of the abdomen whereas 0.3°C was found with the trunk helix. Detailed heating patterns were not determined using the APA because such have been presented earlier for the same phantom [5], [6].

The thigh helix was tested with the phantom-filled mannequin as shown in Fig. 10. The split-tube BALUN was used for all tests made with the thigh helix. A frequency of 51.07 MHz with a forward power of 50 W (0.2 W reflected) was used in these tests. Measurements with the implantable electric field probe showed that the deposition in a small region at the crotch of the mannequin exceeded that within the volume enclosed by the thigh helix. There was an additional problem in that a strong electric field was present in the air space between the helix and the unenclosed (untreated) leg of the mannequin. Using a forward power of only 10 W, the electric field intensity in this air space was as strong as 900 V/M. One of us (P. F. Turner) received a small RF burn when he placed his hand in this region while making the measurements.

Finally, the MAPA was tested with the phantom-filled mannequin as shown in Fig. 11. A frequency of 178.16 MHz with a forward power of 50 W (0.8 W reflected) was used in these tests with the MAPA. No detectable fields were found in the crotch area of the mannequin using the implantable electric field probe. In addition, no measurable fields were found in the air space between the MAPA and the unenclosed (untreated) leg. It appears that the water-filled bolus serves to selectively couple energy to the treated region and thus decreases the coupling to other parts of the mannequin.

V. Measurements of Scattered Fields

The scattered electric and magnetic fields were measured when the trunk helix and APA were used with the phantom-filled mannequin. A Holaday Industries model HI-3002 isotropic broad-band field strength meter was used for these tests.

Values of the scattered electric and magnetic fields determined when the trunk helix was used with the mannequin are presented in Figs. 12 and 13, respectively. The net RF power was 7.7 W (10 W forward, 2.3 W reflected) at a frequency of 70.93 MHz. A split-tube BALUN was used with the trunk helix to provide consistent measurements. Shaded lines at the top, bottom, and side in Fig. 12 represent conducting surfaces of the screen-room. These surfaces were not shown in the subsequent figures, or in Figs. 7 and 8 due to a change in scaling.

Figs. 14 and 15 give the values of the scattered fields determined using the APA with the phantom-filled mannequin. A net RF power of 7.7 W (<0.05 W reflected) was used to facilitate comparison to the values obtained using the truck helix. The frequency was 70.94 MHz. The water-filled bolus was used during these measurements. For comparison, the ANSI guideline for human exposure at the frequencies used in these tests is 4000 V^2/M^2 or 0.025 A^2/M^2.

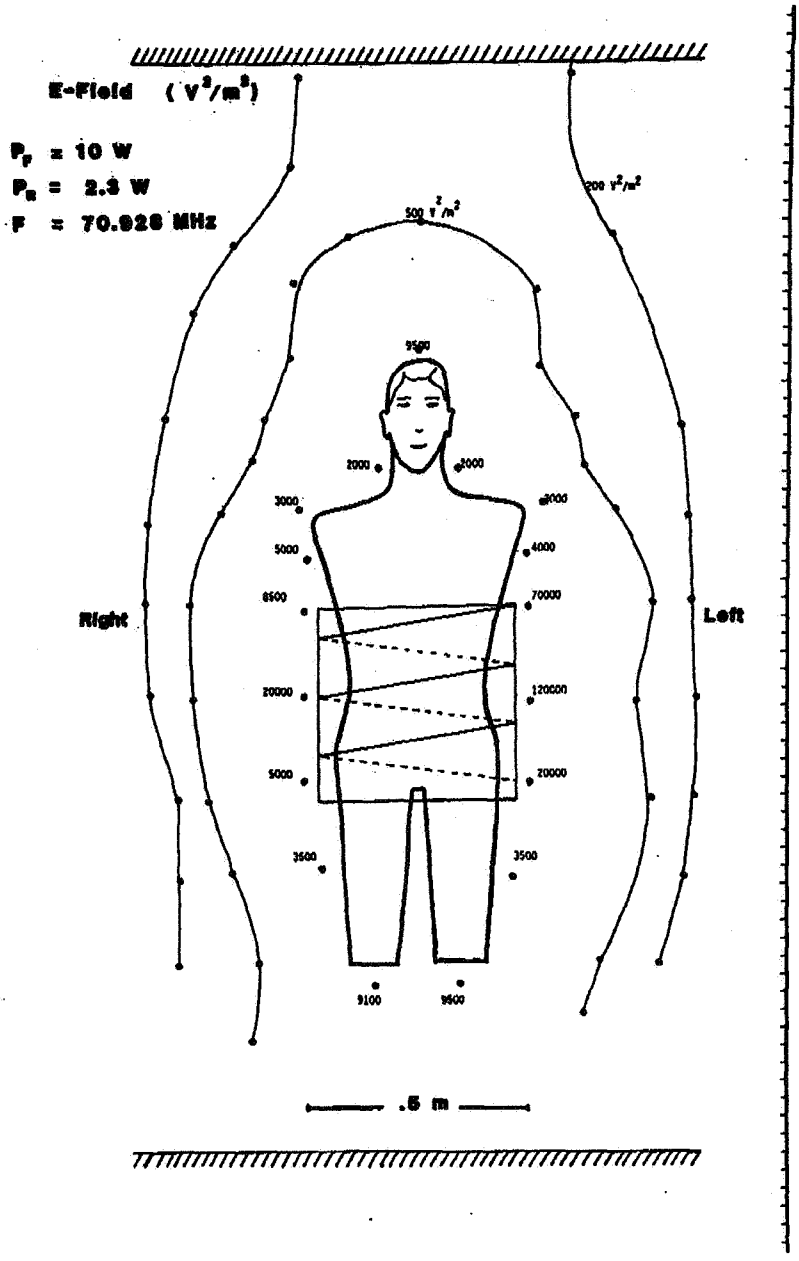

Fig. 12. Scattered electric field with trunk helix.

In most areas, the scattered fields are comparable to the two applicators. The exception is that intense fields, as strong as 120 000 V^2/M^2 and 1.5 A^2/M^2, were measured just outside the trunk helix and the fields were not unusually strong near the outer surface of the APA. These observations of strong fields external to the applicator are consistent with earlier measurements of an intense electric field when the thigh helix was used with the mannequin. Indeed, intense fields should be expected near the conducting surfaces of a helical coil. Exposure to these fields could be avoided by using a dielectric spacer several centimeters in thickness on the inner and outer surfaces of a helical coil applicator. It is anticipated that the fields external to helical coil could be decreased by using a water-filled bolus similar to that used with the APA and MAPA but such an arrangement has not yet been tested.

VI. Conclusions

It is our opinion that the major factor limiting the depth of heating obtained with the two helical coil applicators was the relatively low magnitude of the length to diameter ratios (L/D). In fact, the depth of heating was significantly greater with the thigh helix (L/D = 1.57) than with the trunk helix (L/D = 1.0). Others have claimed good results when using coils having larger L/D values, but they observed highly nonuniform transverse heating with a coil

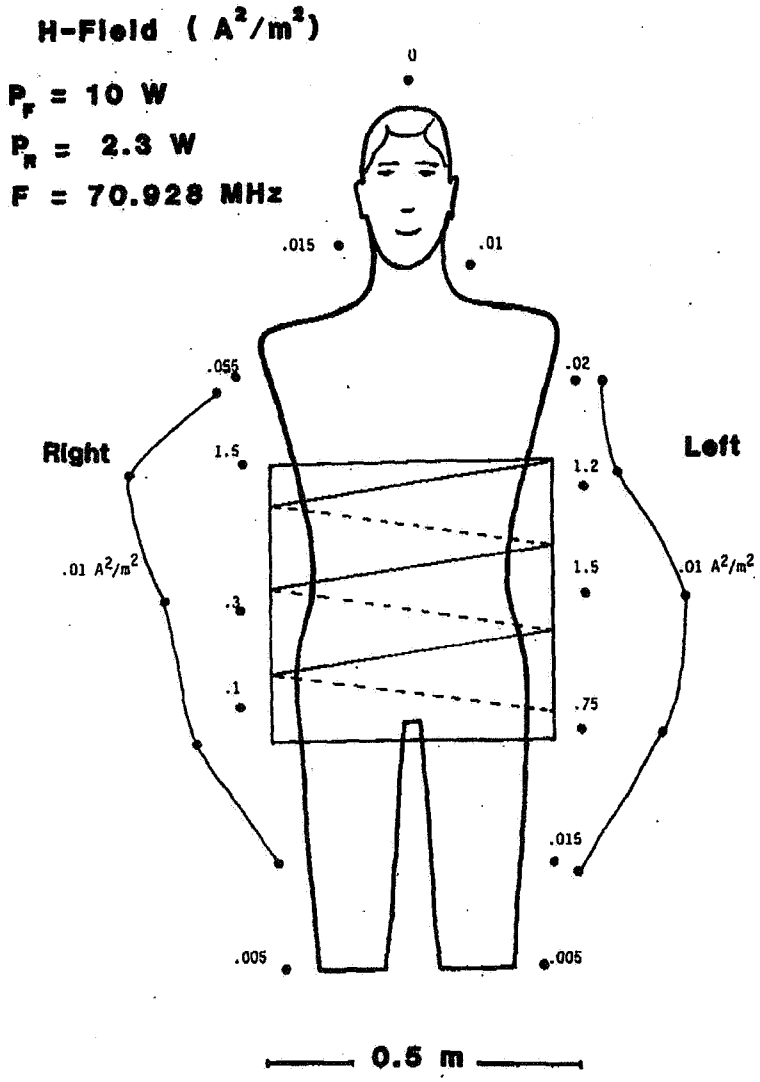

Fig. 13. Scattered magnetic field with trunk helix.

having *L/D* equal to one [2]. The problem is that coils having values of *L/D* significantly greater than those in the present study may be difficult to use for treatment in some regions of the human body. Helical coil applicators should have diameters that are at least equal to those used in the present series of tests in order to avoid highly localized deposition or "hot spots" due to the strong electric field near the turns of the helix. Unfortunately, a helix having a diameter sufficiently large for reasonable clearance from the leg and having the suggested *L/D* ratio of at least 3.0 [16] would necessarily have the point of maximum deposition (the midpoint of the helix) no higher than the knee. Similarly, a helix intended for use with the arm and having the suggested value of *L/D* would have the point of maximum deposition located no higher than the elbow. Substanial deposition would be expected to occur over a major portion of the limb when using such applicators. Such applicators would appear to be inappropriate for the large number of thigh and upper arm cases currently being treated by other modalities. We would also anticipate that a trunk helix having the suggested value of *L/D* would produce heating over a considerable length of the torso, thus increasing the total energy deposited in the body and the amount of unwanted systemic heating.

We do not claim to have fully optimized the values of frequency and pitch angle for the coils which were tested, but such optimization is not likely to cause a substantial increase in the depth of heating since for resonant operation changes in either of the two variables require changes in the other which tend to have compensating effects [4]. We are not aware of attempts by others to optimize helical coil applicators having relatively small values of *L/D*.

Strong fields were measured external to the helical coil applicators, and tests with a phantom-filled mannequin suggest that the genitals could be injured if a helix was used to treat the thigh. It is anticipated that damage to the face could occur if a helix was used to treat the upper arm. It is anticipated that the fields external to a helical coil

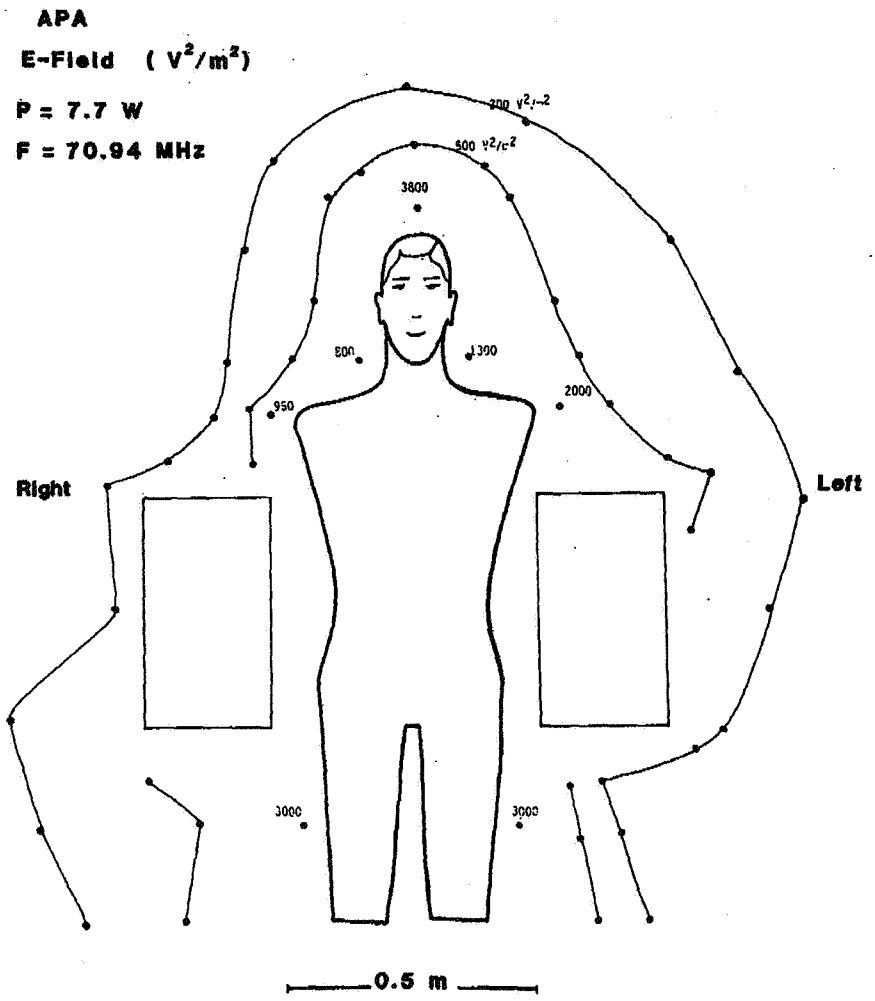

Fig. 14. Scattered electric field with APA.

could be decreased by using a water-filled bolus similar to that used with the APA and MAPA, but such an arrangement has not yet been tested.

By contrast, the BSD APA and MAPA were found to produce deep heating and did not cause strong fields external to the applicators. The absence of azimuthal electric fields with the APA and MAPA is one factor causing them to have greater depth of heating than was observed with the helical coils. Note that when the MAPA was tested with a cylindrical saline phantom, the mean deposition on the axis exceeded that near the surface, a phenomenom which has never been claimed for the helical coils. It is well known that the APA (and MAPA) may be focused to provide greater deposition near the center of a phantom than occurs near the surface [6]. In addition, it is possible to steer the region of maximum deposition by adjusting the phases and magnitudes of the currents fed to the elements of the phased arrays [6]. The water-filled bolus appears to be required for limiting the extent of deposition obtained with the APA and MAPA as well as decreasing the strength of the external fields.

It is possible that the requirement for resonant tuning with a helix could present a problem in clinical usage. Unlike the APA and MAPA, the helical coil applicators are resonant devices and must be operated at a frequency which is dependent upon the loading in addition to the design parameters of the coil. Using all four coil–phantom combinations, we found that the power reflection exceeded 50 percent when the frequency was shifted by more than ± 4 percent of the tuned value.

The authors suggest that phantom-filled mannequins should have greater application in evaluation of systems intended for use in hyperthermia. Several of the phenomena observed in the present work would have been missed if a simpler phantom had been used.

Acknowledgment

Appreciation is extended to L. Calloway, who assisted in the preparation of the helical coils, and R. A. Curtis of OSHA, who helped in the measurement of the scattered fields. The assistance of J-L. Guerquin-Kern in prepara-

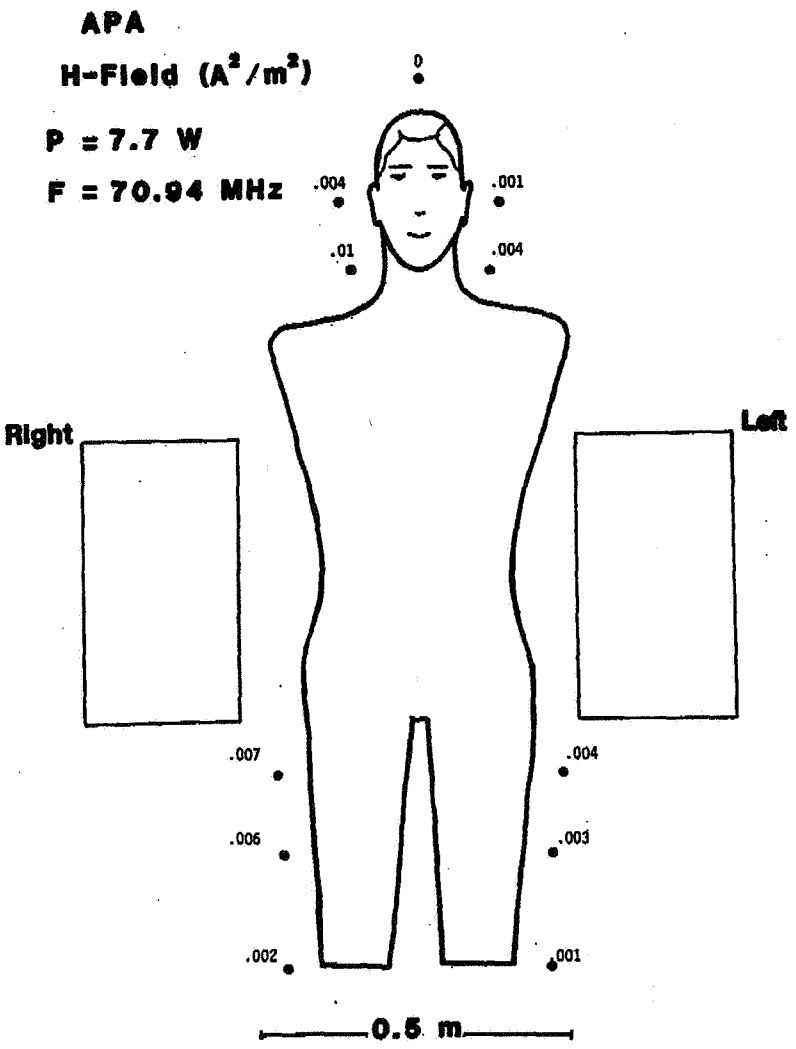

Fig. 15. Scattered magnetic field with APA.

tion of some of the figures is also gratefully acknowledged.

References

[1] J. G. Short and P. F. Turner, "Physical hyperthermia and cancer therapy," *Proc. IEEE*, vol. 68, pp. 133–142, Jan. 1980.

[2] P. S. Ruggera and G. Kantor, "Development of a family of RF helical coil applicators which produce transversely uniform axially distributed heating in cylindrical fat–muscle phantoms," *IEEE Trans. Biomed. Eng.*, vol. BME-31, 98–106, Jan. 1984.

[3] F. S. Chute and F. E. Vermeulen, "A visual demonstration of the electric field of a coil carrying a time-varying current," *IEEE Trans. Educ.*, vol. E-24, pp. 278–283, Nov. 1981.

[4] M. J. Hagmann, "Propagation on a sheath helix in a coaxially layered lossy dielectric medium," *IEEE Trans. Microwave Theory Tech.*, vol. MTT-32, pp. 122–126, Jan. 1984.

[5] P. F. Turner, "Electromagnetic hyperthermia devices and methods," M.S. thesis, *Dep. Elec. Eng.*, Univ. Utah, Salt Lake City, June 1983.

[6] —, "Regional hyperthermia with an annular phased array," *IEEE Trans. Biomed. Eng.*, vol. BME-31, pp. 106–114, Jan. 1984.

[7] —, "Hyperthermia and inhomogeneous tissue effects using an annular phased array," *IEEE Trans. Microwave Theory Tech.*, vol. MTT-32, pp. 874–882, Aug. 1984.

[8] M. J. Hagmann and R. L. Levin, "Coupling efficiency of helical coil hyperthermia applications," *IEEE Trans. Biomed. Eng.*, vol. BME-32, pp. 539–540, July 1985.

[9] D. F. Bowman, "Impedance matching and broadbanding," in *Antenna Engineering Handbook*, H. Jasik, Ed. New York: McGraw-Hill, 1961, ch. 31.

[10] A. Stogryn, "Equations for calculating the dielectric constant of saline water," *IEEE Trans. Microwave Theory Tech.*, vol. MTT-19, pp. 733–736, Aug. 1971.

[11] C. C. Johnson and A. W. Guy, "Nonionizing electromagnetic wave effects in biological materials and systems," *Proc. IEEE*, vol. 60, pp. 692–718, June 1972.

[12] C. H. Durney *et al.*, "Radiofrequency radiation dosimetry handbook," 2nd ed., Univ. Utah, Salt Lake City, SAM-TR-78-22, 1978.

[13] J. W. Strobehn, "Theoretical temperature distributions for solenoidal-type hyperthermia systems," *Med. Phys.*, vol. 9, pp. 673–682, Sept./Oct. 1982.

[14] A. W. Guy, "Analyses of electromagnetic fields induced in biological tissues by thermographic studies on equivalent phantom models," *IEEE Trans. Microwave Theory Tech.*, vol. MTT-19, pp. 205–214, Feb. 1971.

[15] R. L. Bowman, "A probe for measuring temperature in radiofrequency-heated material," *IEEE Trans. Microwave Theory Tech.*, vol. MTT-26, pp. 43–45, Jan. 1976.

[16] P. S. Ruggera, National Center for Devices and Radiological Health, personal communication.

Mark J. Hagmann (S'75–S'78–M'79) was born in Philadelphia, PA, on February 14, 1939. He received the B.S. degree in physics from the Brigham Young University, Provo, UT, in 1960, and the Ph.D. degree in electrical engineering from the University of Utah, Salt Lake City, in 1978. His doctoral dissertation focused on numerical evaluation of the absorption of electromagnetic energy by man.

Subsequent to receiving his doctorate he served as a Research Associate and Research Professor at the University of Utah. He was a Visiting Professor in the Department of Electrical Engineering at the University of Hawaii from 1981 to 1982. Since 1982 he has worked as a Senior Staff Fellow in the Biomedical Engineering and Instrumentation Branch of the Division of Research Services of the National Institutes of Health in Bethesda, MD. His general research interests include numerical procedures for electromagnetics, electromagnetic imaging, biomedical applications of microwaves, and electromagnetic biological effects. Currently he is involved in both theoretical and experimental studies regarding electromagnetic applicators for use in hyperthermia.

Dr. Hagmann is a member of the Bioelectromagnetics Society, the Radiation Research Society, and Sigma Xi. He is the Chairman of the Engineering in Medicine and Biology Society for the Washington, DC, and Northern Virginia chapters and a member of the Executive Committee for the Washington, DC, chapter of the IEEE.

Ronald L. Levin was born in Philadelphia, PA, on January 14, 1951. He received the S.B. (with Honors) and S.M. degrees in mechanical engineering from the Massachusetts Institute of Technology, Cambridge, in 1973 and the Sc.D. degree in mechanical engineering from the Massachusetts Institute of Technology in 1976. His doctoral dissertation dealt with the numerical modeling of the water and solute transport processes associated with the cryopreservation of biological cells at low temperatures.

Subsequent to receiving his doctorate, he served as a Research Fellow for 1 1/2 years in the Biophysical Laboratory of Harvard Medical School. He then was an Assistant Professor for 3 years in the Sibley School of Mechanical and Aerospace Engineering of Cornell University, Ithaca, NY. Since 1981 he has been a Biomedical Engineer in the Biomedical Engineering and Research Branch of the Division of Research Services of the National Institutes of Health in Bethesda, MD, and an Adjunct Assistant Professor in the Department of Biomedical Engineering of the Johns Hopkins School of Medicine, Baltimore, MD. His general research interests include bioheat and mass transfer phenomena and pharmacokinetics. Currently he is involved in both hyperthermia and cryobiology research.

Dr. Levin is a member of the Radiation Research Society, the Cryobiology Society, the American Society of Mechanical Engineering, and the American Institute of Chemical Engineering. He has just completed a term as the Chairman of the ASME Technical Committee on Bio-Heat and Mass Transfer.

Paul F. Turner (S'70–M'79) was born in Salt Lake City, UT, on April 19, 1947. He received the B.S.E.E. degree in 1971 and the M.S.E.E. degree in 1983, both from the University of Utah. He initially specialized in microwave communications and antenna design for defense systems.

In August of 1978 he joined BSD Medical Corporation. Since that time he has devoted full time to the development and design of microwave and RF applicators and methods for the purpose of hyperthermic cancer treatment. He has obtained five patents and several patents are pending related to his work.